Research Article | Vol. 28, No. 15 / 20 July 2020 / Optics Express 22027
Optics EXPRESS

Dynamics of optical injection in an external cavity based FP-LD for wide tunable microwave signal generation

MUYOUNG LEE,[1] BIKASH NAKARMI,[2] AND YONG HYUB WON[1,*]

[1] School of Electrical Engineering, Convergence Optoelectronic Device Engineering Lab, Korea Advanced Institute of Science and Technology, Daejeon 34141, South Korea
[2] Key Laboratory of Radar Imaging and Microwave Photonics, Ministry of Education, Nanjing University of Aeronautics and Astronautics, Nanjing 210016, China
[*] yhwon@kaist.ac.kr

Abstract: In this paper, we analyze the dynamics of optical injection in an external cavity based Fabry-Pérot laser diode (ECFP-LD) for wide tunable microwave signal generation. The ECFP-LD is a specially designed FP-LD that has a self-locked single dominant mode. The injected beam power is varied to analyze the dynamics of optical beam injection on the ECFP-LD. The ECFP-LD shows the interesting behavior of red-shift followed by hopping to another self-injected mode equivalent to FP-LD external and internal cavity modes separation, which provides the fine and coarse tuning of the self-injected mode. The optical beating of the injected beam and the self-injected mode, whether it is the fine red-shifted self-injected mode or the hopped self-injected mode equivalent to the external or internal cavity mode separation, provides a wide tunable range of microwave generation. We obtained fine tuning of 3 GHz for every self-injected mode, and coarse tuning of 15 GHz and 150 GHz, which is equivalent to the free spacing tuning of the external cavity (0.12 nm) and internal FP-LD cavity (1.17 nm), with change in the power of the injected beam. The maximum coarse tuning range is about 3.72 nm, and the corresponding beating frequency tuning range is 330 GHz. Hence, a wide tunable microwave frequency can be obtained by optical beating of the shifted/hopped self-injected mode and the injected beam.

1. Introduction

Photonic approaches for the generation of microwave signals have attracted considerable attention in recent years owing to their many potential applications in wireless communication systems [1–3], photonic radar [4], satellite communication [5], bio-sensors [6], and industrial applications such as waste treatment, dying, structure monitoring and others [7,8]. These techniques offer important advantages in comparison to traditional electronic circuitry. They can be used to realize an EMI-free system with a wide tunable range, high bandwidth, and lower power consumption. In addition, photonic technology not only overcomes the limited frequency response of electronic devices but also transmits microwave signals over long distances by using optical fiber [9]. Thus, photonic microwave signal generation is expected to play a key role in a wide range of future applications.

Various techniques using a variety of optical components, such as modulating RF signals using modulators and optical heterodyning in semiconductor lasers (DFB laser, VCSELs, and FP-LD), have been proposed for the generation of microwave signals [10]. One widely used operating principle for microwave generation is optical injection locking in semiconductor lasers [11–13]. An optically injected semiconductor laser exhibits various dynamic states including stable locking, four-wave mixing (FWM), period-one (P1) oscillation, period-two (P2) oscillation, quasi-periodic oscillation, and chaotic oscillation. Stable locking has been used to stabilize semiconductor lasers for the purposes of modulation bandwidth enhancement, chirp reduction, and noise suppression.

#395141 https://doi.org/10.1364/OE.395141
Journal © 2020 Received 17 Apr 2020; revised 20 Jun 2020; accepted 25 Jun 2020; published 10 Jul 2020

Optics EXPRESS

Non-linear dynamics of P1 oscillation is widely used for a tunable photonics microwave source. While the laser is operating with P1 oscillation, the increase in the injection strength normally decreases the optical gain due to the saturation effect. The cavity resonance is then red-shifted through the antiguidance effect [14]. The maximum red-shift of about 12 GHz with single-beam injection has been reported with change in the injection ratio [15–18]. In addition, P1 oscillation, FWM, and chaotic phenomena have also been analyzed by many researchers. They are used for microwave communication; optical secure communications due to chaotic carriers offer a certain degree of intrinsic privacy in data transmission [19]. Recently, we used an external cavity based FP-LD (ECFP-LD) for the generation of microwave signals ranging from a few GHz to several hundred GHz [20]. The ECFP-LD provides unique properties, including a self-locking mode, low threshold current, high side-mode suppression ratio (SMSR), and simple structure [21]. Due to these advantages, various applications have been realized such as wavelength conversion, optical logic gate, switching, memory, and multi-spectrum RF signals generation [20–25].

In this paper, we investigate an optically injected ECFP-LD for microwave signal generation under the non-linear dynamic P1 oscillation state and demonstrate fine and coarse tuning of the microwave signal for the first time, which is not available in other single mode semiconductor lasers. The power of the external beam is controlled to change the gain curve, wavelength shift and mode hopping of the ECFP-LD, which provides the tunability of microwave signal. Because we used the ECFP-LD for the analysis and the generation of microwave signals, besides the red-shift phenomena, hopping of the self-injected mode (SM) due to the free spectral range of the external and internal cavity modes, coarse tuning of microwave signal with frequency of 15 GHz and 150GHz, respectively, can be obtained. The fine and coarse tuning of the ECFP-LD with different SMs is also analyzed and used for the generation of microwave signals with a wide tuning frequency. Also, we demonstrate the tuning of the SM by changing the injected optical beam power, thus overcoming many limitations of the conventional tunable laser, such as a complicated driving system that either adjusts the external cavity length optically by varying the operating temperature or the biasing current or physically adjusting the distance to the mirror or producing stress/strain [26–31]. Therefore, it is not necessary to change the bias current or temperature to tune the SM of the ECFP-LD while operating under the P1 oscillation state.

Taking advantage of the P1 oscillation state of the ECFP-LD and the phenomena of SM hopping due to external and internal cavity mode with change in the power of the injected beam, we proposed an optical microwave oscillator which exhibits a wide tunability of RF signal from a few GHz to several hundred GHz by simply changing the power of the external injected beam. In addition, we investigate the gain shift and SM hopping phenomena of the ECFP-LD due to variation in injection beam power, and the coarse and fine frequency tunability of microwave oscillator depending on the characteristics of the ECFP-LD.

2. Operation principle and experimental setup

The FP-LD used in the proposed scheme was specially designed and developed by modifying a commercially available multi-mode Fabry Pérot laser diode (MMFP-LD) that has multi-mode spectrum output under a normal biasing condition and a free spectral range (FSR) of 1.17 nm. The ECFP-LD can be obtained by eliminating the inclinations of 6° to 8° of the coupling fiber present in conventional FP-LDs, which forms an external cavity that provides only one single longitudinal mode with high amplitude, suppressing other side modes present in MMFP-LD. The self-locking mode can be tuned to another wavelength by varying the operation temperature, and it is the tunable over a wide range of about 10 nm. The ECFP-LD exhibits characteristics similar to those of a multi-mode FP-LD, including power stability, wavelength stability, and mechanical stability. The ECFP-LD used for the experiment has two cavity modes, namely, the internal cavity mode of the FP-LD and the external built-in cavity mode, as illustrated in Fig. 1. The FSR

Optics EXPRESS

of a cavity is expressed as

$$\Delta\lambda_{FSR} = \lambda^2/2nl \tag{1}$$

where λ is the wavelength of the longitudinal mode, n is the refractive index of an active medium within the cavity, and l is the length of the cavity. The internal cavity mode has a relatively large FSR of 1.17 nm, which is determined by the quantum well cavity length of the FP-LD of 300 μm. The external cavity, on the other hand, has a relative short FSR of 0.12 nm due to the external cavity length of 4 mm. By properly adjusting the temperature or bias current, a mode-matching condition is achieved from both cavities for SM oscillation [21]. In this experiment, high power injection with negative wavelength detuning was mainly used for the P1 oscillation state. In negative wavelength detuning injection locking, we observe four main stages: (1) weak injection locking in which the SM is not suppressed; (2) moderate injection locking in which the side mode gains sufficient power without suppressing the SM; (3) strong injection locking in which the SM is suppressed but the injected beam and the side mode beam still exist; and (4) ultra-high injection locking in which the red-shift occurs and only the injected beam exists, similar to positive wavelength detuning, which is well discussed in our previous research [25]. In [25], the analysis of red-shift and the phenomena beyond the ultra-high injection locking stage, where injection locking with the suppression of the beams is obtained, is not analyzed. It can be further used for the wide tunability of RF signal generation. On increasing the power of the injected beam beyond state 4, ultra-high injection locking, the ECFP-LD shows important characteristics of mode hopping of the self-injected beam. Beyond state 4, increasing the injection strength, red-shift originates from the antiguidance effect due to the reduction in the average charge carrier density and optical gain, and it is caused by the saturation effect of optical injection. On varying the power of the injection beam, the refractive index of the active region of the ECFP-LD changes according to average charge carrier density. As the intensity of the injected beam increases, more charge carriers are consumed, reducing the average charge carrier density and increasing the refractive index. Thus, the gain curve and all of the FP-LD cavity modes are red-shifted simultaneously. As a result, a SM oscillates under optimal mode-matching conditions between the external cavity mode and FP-LD mode is achieved, as illustrated in Fig. 1. With the increase in the power of the external beam, the SM of the ECFP-LD is continuously red-shifted without suppression of the SM within a matching limit of about 0.025 nm between the external cavity mode and the FP-LD mode. Therefore, the optical beating of the SM of the ECFP-LD which is continuously red-shifted, and a fixed external injection beam continuously generate a frequency varying microwave signal with fine adjustment of the power of the injected beam. When the power of the injected beam is increased beyond the red-shift of the SM, the SM vanishes as the mode matching condition is broken for that particular wavelength; therefore, mode competition occurs for the next SM. The hopping of SM to another mode of the FP-LD internal cavity or external cavity modes enables coarse tuning of microwave generation whereas the red-shift of each SM enables fine tuning of the microwave generation.

The experimental setup for the analysis of the P1 oscillation state in the ECFP-LD and the tuning capability is shown in Fig. 2. The ECFP-LD had a self-injected single longitudinal mode with a side-mode suppression ratio (SMSR) of more than 30 dB, which was achieved by controlling the operating temperature and biasing current of the ECFP-LD through the laser driver. A tunable laser diode was used to inject an external light beam into the ECFP-LD. The external beam could be injected into any of the side modes in the ECFP-LD, including the free-running self-injected mode (FRSM) for negative wavelength detuning. An erbium-doped fiber amplifier (EDFA) was used to amplify and control the power of the external injected beam from 0 mW to 18 mW. The amplified external beam was divided into two branches with a 10:90 optical coupler (OC); the 10% intensity was fed to a photometer to measure the power of the injected beam, and the 90% intensity was injected into the ECFP-LD. The external beam was injected into the ECFP-LD via a polarization controller (PC) because gain modulation in the ECFP-LD would

Optics EXPRESS

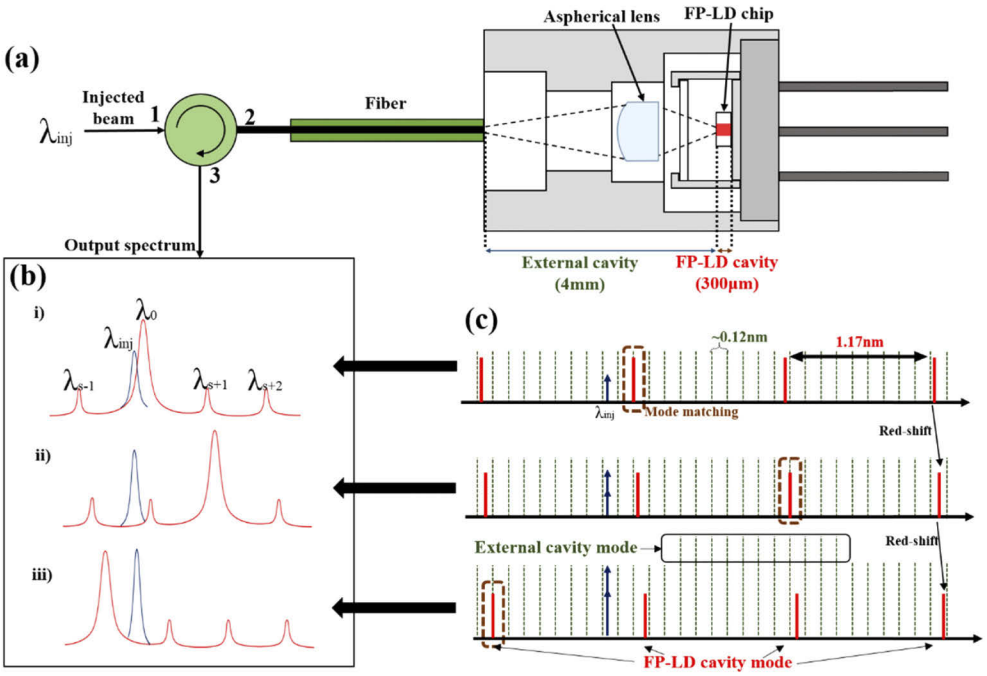

Fig. 1. Schematic illustration of (a) ECFP-LD with a built-in external cavity configuration, (b) resulting spectrum, and (c) external cavity mode and FP-LD mode matching condition depends on intensity of injection beam.

only work in the TE mode of the injected beam. To analyze the spectral output of the ECFP-LD in the optical and electronic domains, a 50:50 coupler (CO) was used and measured by an optical spectrum analyzer (OSA) set with 0.05 nm resolution and an electrical spectrum analyzer (ESA) along with a photodiode (PD) of 40GHz bandwidth.

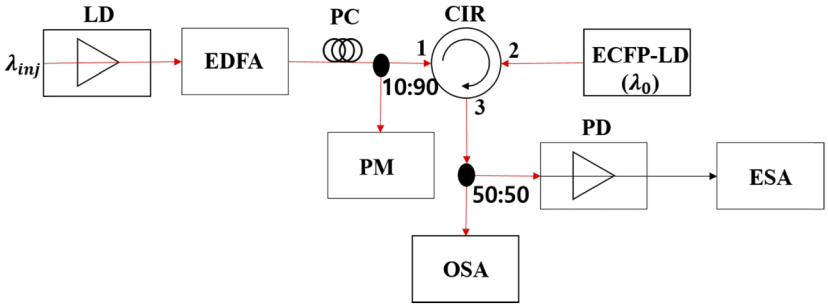

Fig. 2. Experimental setup of the proposed the tunable microwave oscillator. LD: laser diode; EDFA: erbium-doped fiber amplifier; PC: polarization controller; CIR: optical circulator; PM: photometer; OSA: optical spectrum analyzer; PD: photodiode; ESA: Electrical spectrum analyzer.

3. Experimental results and discussion

At first, we observed and analyzed the P1 oscillation state by injecting an external beam into the FRSM of the ECFP-LD [14]. The ECFP-LD operated at a bias current of 22 mA and

Optics EXPRESS

21.9°C operation temperature, with a threshold current of 12 mA. Under these conditions, the self-emission mode of the ECFP-LD had the wavelength and the output power of 1550.75 nm and 0.41 mW, respectively, providing an SMSR of 33.2 dB. The power of the external beam was controlled by the EDFA when an external beam was injected into the left side of the FRSM of the ECFP-LD with negative wavelength detuning of -0.13 nm. Figure 3(a) shows the variation in wavelength and output power of the FRSM of the ECFP-LD with increasing external injected beam power from 0 mW to 18 mW. Here, $\lambda_0(\uparrow)$ and $\lambda_0(\downarrow)$ indicate the wavelength of the FRSM when the power of the external injected beam power increased, $P_{\lambda inj}(\uparrow)$ and decreased, $P_{\lambda inj}(\downarrow)$, respectively. We observed that the change in the wavelength shift was gradually increased with the change in the power of the injected beam from 9 mW to 18 mW. While the total wavelength shift of the FRSM was about 0.365 nm, it was equal to the total gain shift and the total amount of any individual FP-LD mode shift. The injection locking hysteresis occurs in the external injection beam power range from 3 mW to 6 mW, as presented in the previous paper [25], but beyond 9 mW, the P1 oscillation state hardly shows hysteresis as seen in Fig. 3(a). Figure 3(b-i) shows the change in the power of the output beam as a function of injected beam power, which is caused by the gain shift. Here, λ_0 indicates the wavelength of the FRSM and λ_{s-1}, λ_{s+1}, and λ_{s+2} indicate the -1^{st}, $+1^{st}$, and $+2^{nd}$ side modes of the ECFP-LD, respectively. It is clearly seen that below 9 mW, the increase in external beam power, the ECFP-LD changes from weak to moderate, to high injection locking stages as mentioned before, but the wavelength of the FRSM hardly changes. However, when the power of the external injected beam is beyond 9mW, the injected beam energy mainly contributes to the P1 oscillation state. Therefore, a unique property of the ECFP-LD, SM hopping, is observed. Different side modes of the ECFP-LD become self-injected with change in the power such as in order of λ_0, λ_{s+1}, λ_{s+2}; λ_{s-1}, λ_0, λ_{s+1}, λ_{s+2}; λ_{s-1}, λ_0, λ_{s+1}, λ_{s+2}; λ_{s-1}, and λ_0.

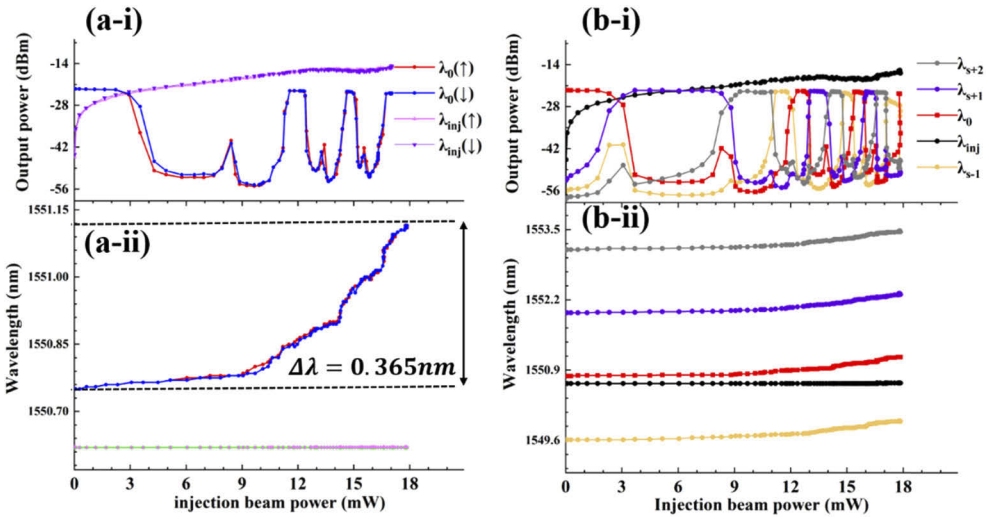

Fig. 3. The characteristics of ECFP-LD with negative wavelength detuning optical injection. (a) Hysteresis of free-running self-injected mode, (b) The output powers and wavelengths as function of injection beam power.

A fine red-shift of about 3 GHz for each SM is also observed in the interval of the injected beam power, as shown in Fig. 3(b-ii). The mode hopping occurs as matching of the FP-LD mode, and the external cavity mode changes according to the intensity of the external injected beam. As seen in Fig. 3, as the injection beam power increases, the output power of each mode increases or decreases. This indicates that the SM of the ECFP-LD is hopping to another FP-LD cavity mode. This mode hopping occurs because the external cavity mode and FP-LD mode matching and

Optics EXPRESS

mismatching are repeated during the red-shift caused by the increasing power of the external injected beam. The matched mode shows SM oscillation with a high-side mode suppression ratio when one of the FP-LD mode wavelengths is the same as that of the external cavity mode. On the other hand, the mismatched modes of the FP-LD are suppressed; thus, coarse tuning is possible. Coarse tuning is achieved with the tuning ranges of 0.12 nm and 1.17 nm, which are exactly the same as the FSR of the external cavity mode and the FP-LD cavity mode, respectively. The SM, which is created by matching of the external cavity mode and FP-LD mode, is continuously red-shifted about 3 GHz with increasing external beam power, as shown in more detail in Fig. 4.

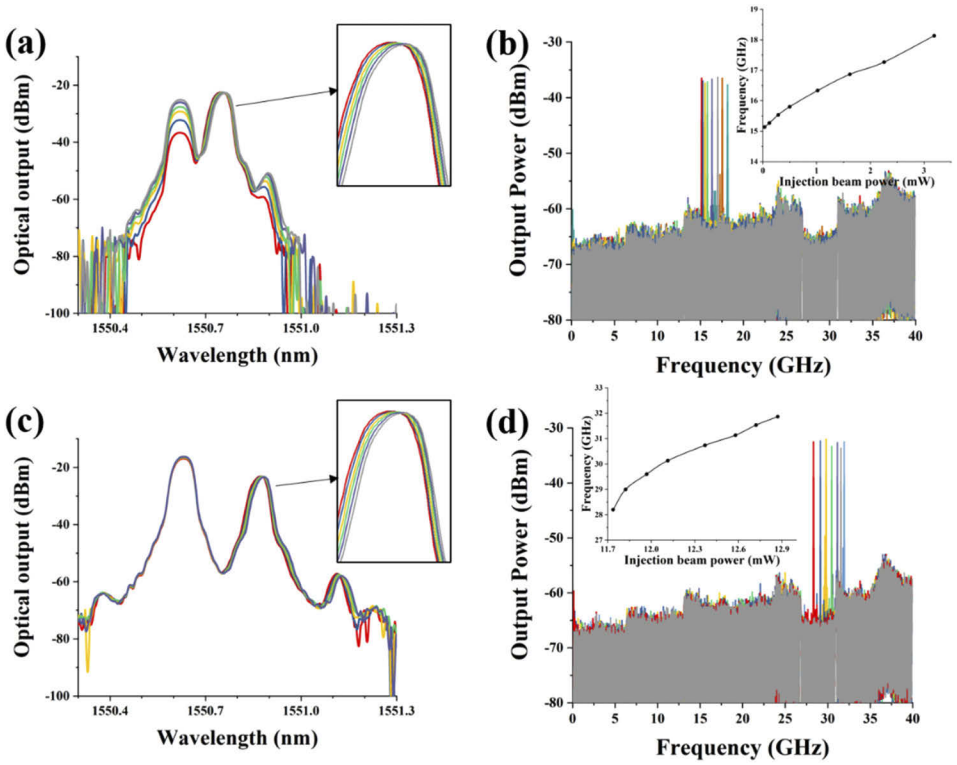

Fig. 4. Continuously tunable microwave signal generation (fine tuning) (a), (c) continuously shifted self-injected mode. (b), (d) Microwave signal generated by optical beating of external injected beam and corresponding self-injected mode, respectively.

In Fig. 4(a), the SM is continuously red-shifted as the power of the injected beam changes from 0 mW to 3.2 mW. The total red-shift of 0.025 nm is observed in OSA, which is shown in the inset clearly. Figure 4(b) shows the electrical spectrum of the RF signal, which was obtained from heterodyning of the injection beam and the red-shifted SM. The total red-shift of 3.07 GHz (15.06 GHz to 18.13 GHz) is observed in the electric domain result, which is equivalent to the wavelength shift of the self-injected beam 0.025 nm (1550.75 nm to 1550.775 nm). The red-shift on SM in this first scenario is considered fine wavelength (frequency) tuning. In the second scenario, further increasing the power of the injected beam, hopping of the SM to another mode occurs due to the internal cavity mode. As a result, the wavelength difference between the injected beam and the SM varies, and the RF generation changes with higher frequency changes by about 150 GHz, which we consider coarse tuning. With increasing power of the injected beam, we observe not only mode hopping of the FRSM but also return to the previous mode with a frequency difference of about 15 GHz (15.06 GHz shift to 28.2 GHz) in this third scenario. The

Optics EXPRESS

red-shift of 3.57 GHz (28.2 GHz to 31.77 GHz) is also observed with increasing power of the injected beam from 11.8 mW to 13 mW, as shown in Figs. 4(c)–4(d). The signal-to-noise ratios of the output RF signals are above 23 dB and 26 dB with fine tuning ranges of 3.07 GHz and 3.57 GHz, respectively. The shifting of the FRSM to other modes can be observed with increasing power of the injected beam and further red-shift of each SM, as shown in Fig. 5.

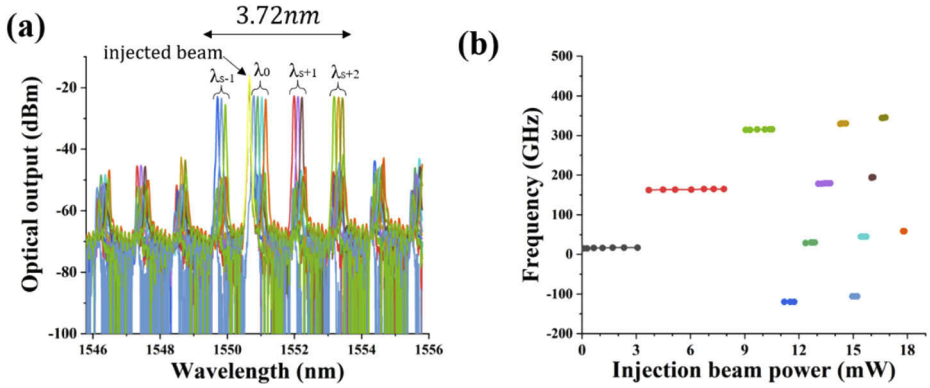

Fig. 5. (a) Optical spectrum of self-injected mode oscillation at various external injected beam power. (b) Microwave frequency generated by optical beating of injected beam and corresponding self-injected mode as a function of injection beam power.

In Fig. 5(a), the wavelengths of SMs with an SMSR of at least 20 dB with various conditions of external injected beam power are shown. Mode hopping of the SM occurs in the order of 1550.75 nm (λ_0), 1551.94 nm (λ_{s+1}), 1553.15 nm (λ_{s+2}), 1549.67 nm (λ_{s-1}), 1550.86 nm (λ_0), 1552.06 nm (λ_{s+1}), 1553.27 nm (λ_{s+2}), 1549.79 nm (λ_{s-1}), 1550.99 nm (λ_0), 1552.18 nm (λ_{s+1}), 1553.39 nm (λ_{s+2}), 1549.91 nm (λ_{s-1}), and 1551.1 nm (λ_0) successively as the injected beam power increases from 0 mW to 18 mW, respectively. The mode hopping occurs about 1.17 nm and 0.12 nm; these values are consistent with the FSR of the FP-LD cavity mode and external cavity mode. Therefore, the total wavelength shift range of the SM is 3.72 nm, which is from 1549.67 nm to 1553.39 nm. As seen in Fig. 5(b), the total of twelve instances of mode hopping occur with variation of the power of the injected beam from 0 mW to 18 mW. The beating frequency tuning range corresponding to wavelength shift with change in the power of the injected beam is 330 GHz, which is from 16 GHz to 346 GHz as shown in Fig. 5(b). Moreover, it is worth noting that every hopping mode shows 3 GHz of red-shift with fine change in the power of the injected beam as seen in Fig. 4. Thus, it is possible to provide coarse tuning of 15 GHz and 150 GHz limited to 3.72 nm as well as fine tuning within the range of 3 GHz of microwave signal frequencies in the P1 oscillation state. In this experiment, the maximum tuning of 3.72 nm with change in the power of the injected beam was limited due to the gain saturation of the EDFA. However, it is expected that more wavelength shifting can be obtained by injecting an external beam with higher power, which would be similar to mode hopping with control of the bias current and operating temperature [21].

4. Conclusion

In conclusion, we analyzed the dynamic behavior of optical injection in an ECFP-LD, especially in P1 oscillation with negative wavelength detuning. The red-shift on the FRSM and shift in the SM with change in the power of the injected beam was observed. We demonstrated a unique behavior of mode hopping of the SM and returning to the previous mode with the wavelength difference of 0.12 nm compared to the previous mode of the ECFP-LD on injection of an external beam. This is due to the external cavity mode, which is not available in other single-mode

Optics EXPRESS

semiconductor lasers. This unique feature allows fine tuning and coarse tuning of the output frequency by optical beating of the SM and the injected beam. The fine tuning is due to the red-shift whereas the coarse tuning of 15 GHz and 150 GHz is due to the mode shifting to the external cavity and mode hopping to another mode of the FP-LD cavity, respectively. The fine tuning range of about 0.025 nm, which is determined by mode matching-limit between the FP-LD cavity mode and the external cavity mode, was observed experimentally. Fine tuning of about 3 GHz was observed for every SM; it was achieved by changing the power of the injected beam. Coarse tuning occurs discontinuously due to the mode hopping between cavity modes. The intervals of coarse tuning are about 1.17 nm and 0.12 nm, which are equal to the FSR of the FP-LD cavity mode and the FSR of the external cavity mode, respectively. The total shift of 3.72 nm was obtained in the ECFP-LD with the power variation of 18 mW, whereas the shift of about 0.365 nm was observed for every FP-LD mode. The limitation of the total shift to 3.72 nm is due to the limitation of the amplification power, which we believe can be increased on increasing the injected beam power. The obtained experimental results can be used to guide the generation of a single/multiple linear frequency modulation (LFM) signal with various center frequencies, which can be used for object detection techniques for radar.

Disclosures

The authors declare that there are no conflicts of interest related to this article.

References

1. H. Shames, M. J. Fice, K. Balakier, C. C. Renaud, F. van Dijk, and A. J. Seed, "Photonic generation for multichannel THz wireless communication," Opt. Express **22**(19), 23465–23472 (2014).
2. R. Waterhouse and D. Novack, "Realizing 5G: Microwave photonics for 5G mobile wireless systems," IEEE Microw. Mag. **16**(8), 84–92 (2015).
3. I. K. Akyildiz, J. M. Jornet, and C. Han, "Terahertz band: Next frontier for wireless communications," Phys. Commun. **12**, 16–32 (2014).
4. P. Ghelfi, F. Laghezza, F. Scotti, G. Serafino, A. Capria, S. Pinna, D. Onori, C. Porzi, M. Scaffardi, A. Malacarne, V. Vercesi, E. Lazzeri, F. Berizzi, and A. Bogoni, "A fully photonics-based coherent radar system," Nature **507**(7492), 341–345 (2014).
5. S. Pan, D. Zhu, S. Liu, K. Xu, Y. Dai, T. Wang, J. Liu, N. Zhu, Y. Xue, and N. Liu, "Satellite payloads pay off," IEEE Microw. Mag. **16**(8), 61–73 (2015).
6. P. H. Siegel, "Terahertz technology in biology and medicine," IEEE Trans. Microwave Theory Tech. **52**(10), 2438–2447 (2004).
7. T. C. S. Girisun and C. Babeela, "Extraction of Fe2O3 from the Industrial Waste for Photonic Applications," Synth. React. Inorg., Met.-Org., Nano-Met. Chem. **44**(8), 1221–1224 (2014).
8. E. Schlosser, J. Wolfrum, L. Hildebrandt, H. Seifert, B. Oser, and V. Ebert, "Diode laser based in situ detection of alkali atoms: development of a new method for determination of residence-time distribution in combustion plants," Appl. Phys. B **75**(2-3), 237–247 (2002).
9. C. T. Tsai, C. H. Lin, C. T. Lin, Y. C. Chi, and G. R. Lin, "60-GHz Millimeter-wave Over Fiber with Directly Modulated Dual-mode Laser Diode," Sci. Rep. **6**(1), 1–12 (2016).
10. J. Yao, "Microwave photonics," J. Lightwave Technol. **27**(3), 314–335 (2009).
11. L. Goldberg, H. F. Taylor, J. F. weller, and D. M. Bloom, "Microwave signal generation with injection-locked laser diodes," Electron. Lett. **19**(13), 491–493 (1983).
12. J. Zhou, X. Feng, Y. Wang, Z. Li, and B. Guan, "Dual-wavelength single-frequency fiber laser based on FP-LD injection locking for millimeter wave generation," Opt. Laser Technol. **64**, 328–332 (2014).
13. A. Hurtado, I. D. Henning, M. J. Adams, and L. F. Lester, "Generation of Tunable Millimeter-Wave and THz Signals With an Optically Injected Quantum Dot Distributed Feedback Laser," IEEE Photonics J. **5**(4), 5900107 (2013).
14. J. Ohtsubo, Semiconductor lasers: stability, instability and chaos (Springer, 2012).
15. S. C. Chan, "Analysis of an Optically Injected Semiconductor Laser for Microwave Generation," IEEE J. Quantum Electron. **46**(3), 421–428 (2010).
16. K. H. Lo, S. K. Hwang, and S. Donati, "Optical feedback stabilization of photonic microwave generation using period-one nonlinear dynamics of semiconductor lasers," Opt. Express **22**(15), 18648–18661 (2014).
17. S. Ji, Y. Hong, P. S. Spencer, J. Benedikt, and I. Davies, "Broad tunable photonic microwave generation based on period-one dynamics of optical injection vertical-cavity surface-emitting lasers," Opt. Express **25**(17), 19863–19871 (2017).
18. H. Luo, Y. Jiang, R. Dong, Y. Zi, X. Zhang, and J. Tian, "A Tunable Single-Mode All-Optical Microwave Oscillator by Using Period-One Oscillation in DFB-LD," IEEE Photonics Technol. Lett. **31**(6), 491–494 (2019).

Optics EXPRESS

19. A. Argyris, D. syvridis, L. Larger, V. Annovazzi-Lodi, P. Colet, I. Fischer, J. Garcia-Ojalvo, C. R. Mirasso, L. Pesquera, and K. A. Shore, "Chaos-based communications at high bit rates using commercial fibre-optic links," Nature **438**(7066), 343–346 (2005).
20. B. Nakarmi, S. Pan, and Y. H. Won, "Simultaneous Generation of Multiband Signals Using External Cavity-Based Fabry–Perot Laser Diode," IEEE Trans. Microwave Theory Tech. **66**(1), 606–617 (2018).
21. Y. D. Jeong, Y. H. Won, S. O. Choi, and J. H. Yoon, "Tunable single-mode Fabry–Perot laser diode using a built-in external cavity and its modulation characteristics," Opt. Lett. **31**(17), 2586–2588 (2006).
22. B. Nakarmi, M. Rakib-Uddin, T. Q. Hoai, and Y. H. Won, "Demonstration of All-Optical NAND Gate Using Single-Mode Fabry–Pérot Laser Diode," IEEE Photonics Technol. Lett. **23**(4), 236–238 (2011).
23. B. Nakarmi, T. Q. Hoai, Y. H. Won, and X. Zhang, "Short-pulse controlled optical switch using external cavity based single mode Fabry-Pérot laser diode," Opt. Express **22**(13), 15424–15436 (2014).
24. Y. D. Jeong, J. S. Cho, Y. H. Won, H. J. Lee, and H. Yoo, "All-optical flip-flop based on the bistability of injection locked Fabry-Perot laser diode," Opt. Express **14**(9), 4058–4063 (2006).
25. H. Chen, B. Nakarmi, M. R. Uddin, and S. Pan, "Optical Behavior Analysis of Negative Wavelength Detuning in SMFP-LD and Its Effect on Multi-RF Generation," IEEE Photonics J. **11**(1), 1–9 (2019).
26. J. Hult, I. Burns, and C. Kaminski, "High repetition-rate wavelength tuning of an extended cavity diode laser for gas phase sensing," Appl. Phys. B **81**(6), 757–760 (2005).
27. X. M. Zhang, A. Q. Liu, D. Y. Tang, and C. Lu, "Discrete wavelength tunable laser using microelectromechanical systems technology," Appl. Phys. Lett. **84**(3), 329–331 (2004).
28. J. D. Merlier, K. Mizutani, S. Sudo, K. Naniwae, Y. Furushima, S. Sato, K. Sato, and K. Kudo, "Full C-band external cavity wavelength tunable laser using a liquid-Crystal-based tunable mirror," IEEE Photonics Technol. Lett. **17**(3), 681–683 (2005).
29. W. Y. Oh, S. H. Yun, G. J. Tearney, and B. E. Bouma, "115 kHz tuning repetition rate ultrahigh-speed wavelength-swept semiconductor laser," Opt. Lett. **30**(23), 3159–3161 (2005).
30. H. Cheng, W. Wang, Y. Zhou, T. Qiao, W. Lin, Y. Guo, S. Xu, and Z. Tang, "High-repetition-rate ultrafast fiber lasers," Opt. Express **26**(13), 16411–16421 (2018).
31. L. Levin, "Mode-hop-free electro-optically tuned diode laser," Opt. Lett. **27**(4), 237–239 (2002).